THE JOURNAL OF BIOLOGICAL CHEMISTRY
Vol. 278, No. 36, Issue of September 5, pp. 33809–33817, 2003
Printed in U.S.A.


# Transgenic Overexpression of the $Ca^{2+}$-binding Protein S100A1 in the Heart Leads to Increased *in Vivo* Myocardial Contractile Performance*

Received for publication, February 19, 2003, and in revised form, May 13, 2003
Published, JBC Papers in Press, May 30, 2003, DOI 10.1074/jbc.M301788200

**Patrick Most,[a,b] Andrew Remppis,[a,b] Sven T. Pleger,[a,c] Eva Löffler,[a] Philipp Ehlermann,[a] Juliane Bernotat,[a,c] Christiane Kleuss,[d] Jörg Heierhorst,[e] Patricia Ruiz,[f] Henning Witt,[f] Peter Karczewski,[g] Lan Mao,[h] Howard A. Rockman,[h] Sandra J. Duncan,[i] Hugo A. Katus,[a,j] and Walter J. Koch[i,j,k]**

*From the [a]Medizinische Universitätsklinik und Poliklinik III, Universität zu Heidelberg, 69115 Heidelberg, the [d]Institut für Pharmakologie, Freie Universität Berlin, 14195 Berlin, [e]St. Vincent's Institute of Medical Research and Department of Medicine, St. Vincent's Hospital, The University of Melbourne, Fitzroy, Victoria 3065, Australia, [f]Max Planck Institut für Molekulare Genetik, 14195 Berlin, [g]Max-Delbrück Zentrum, Berlin-Buch, 13125 Berlin, and the Departments of [h]Medicine (Cardiology) and [i]Surgery, Duke University Medical Center, Durham, North Carolina 27710*

**S100A1, a $Ca^{2+}$-sensing protein of the EF-hand family, is most highly expressed in myocardial tissue, and cardiac S100A1 overexpression *in vitro* has been shown to enhance myocyte contractile properties. To study the physiological consequences of S100A1 *in vivo*, transgenic mice were developed with cardiac-restricted overexpression of S100A1. Characterization of two independent transgenic mouse lines with ~4-fold overexpression of S100A1 in the myocardium revealed a marked augmentation of *in vivo* basal cardiac function that remained elevated after β-adrenergic receptor stimulation. Contractile function and $Ca^{2+}$ handling properties were increased in ventricular cardiomyocytes isolated from S100A1 transgenic mice. Enhanced cellular $Ca^{2+}$ cycling by S100A1 was associated both with increased sarcoplasmic reticulum $Ca^{2+}$ content and enhanced sarcoplasmic reticulum $Ca^{2+}$-induced $Ca^{2+}$ release, and S100A1 was shown to associate with the cardiac ryanodine receptor. No alterations in β-adrenergic signal transduction or major cardiac $Ca^{2+}$-cycling proteins occurred, and there were no signs of hypertrophy with chronic cardiac S100A1 overexpression. Our findings suggest that S100A1 plays an important *in vivo* role in the regulation of cardiac function perhaps through interacting with the ryanodine receptor. Because S100A1 protein expression is down-regulated in heart failure, increasing S100A1 expression in the heart may represent a novel means to augment contractility.**

In cardiac muscle, $Ca^{2+}$ signaling plays a major role in the regulation of the contraction and relaxation cycle. Cardiac myocytes contain specific sensors such as troponin C, a $Ca^{2+}$-binding protein of the EF-hand type, that can detect the rise in intracellular $Ca^{2+}$ and initiate the development of active tension (1). S100A1, another EF-hand $Ca^{2+}$-binding protein and a member of the S100 protein family, may also be important in cardiovascular physiology because it is highly expressed in cardiac myocytes and is the most abundant S100 protein in the heart (2). Interestingly, we have previously found that S100A1 appears to be distributed according to compartmental workloads, with highest protein levels in the left ventricle (LV)[1] and progressively lower levels in the right ventricle (RV) and the atria (3). Other studies have revealed a co-localization of S100A1 with the sarcoplasmic reticulum (SR) and the contractile apparatus in myocardium (4). Moreover, *in vitro* studies have shown that S100A1 can interact with numerous intracellular target proteins such as exo- and endoskeletal proteins, metabolic enzymes, signaling molecules, and transcription factors (for review see Ref. 5).

Despite these myocardial localization and *in vitro* studies, a specific *in vivo* role for S100A1 in the heart and cardiac physiology has remained elusive. Recent *in vitro* studies from our group in myocytes and myocardial tissue preparations have identified S100A1 as a novel cardiac inotropic factor and a regulator of myocardial contractility (6, 7). Adenoviral-mediated overexpression of S100A1 protein in cellular cardiac preparations *in vitro* resulted in marked increases in the rate of contraction and relaxation that was associated both with increased intracellular $Ca^{2+}$ transients and decreased $Ca^{2+}$ sensitivity of cardiac myofilaments (6). Interestingly, heart failure, a state in which S100A1 has been found to be significantly down-regulated (3, 8), is characterized by impaired cardiac contractility and diminished $Ca^{2+}$ transients as well as increased $Ca^{2+}$ sensitivity of myofilaments (9–11). In contrast to what was found in the chronically failing heart, S100A1 protein expression was found to be significantly up-regulated in compensated cardiac hypertrophy (12), suggesting that the plastic-

* This work was supported in part by Forschungsförderung Medizinische Fakultät der Universität Heidelberg Grants 93/2002 and 61/2003 (to P. M.), the Deutsche Forschungsgemeinschaft (Re 1083/1-1, to A. R.), the National Institutes of Health (R01 HL56205 and R01 HL61690, to W. J. K.), and the National Health and Research Council of Australia (ID 156705 and ID 205305, to J. H.). The costs of publication of this article were defrayed in part by the payment of page charges. This article must therefore be hereby marked "*advertisement*" in accordance with 18 U.S.C. Section 1734 solely to indicate this fact.

[b] Both authors contributed equally.

[c] Supported by the Boehringer Ingelheim Stiftung.

[j] Both authors contributed to and supported this study equally.

[k] To whom correspondence should be addressed: Dept. of Surgery, Duke University Medical Center, Box 2606, Durham, NC 27710. Tel.: 919-684-3007; Fax: 919-684-5714; E-mail: koch0002@mc.duke.edu.

[1] The abbreviations used are: LV, left ventricle; RV, right ventricle; SV, simian virus; SR, sarcoplasmic reticulum; NLC, nontransgenic littermate control; DHPR, dihydropyridine receptor; RyR, ryanodine receptor; CSQ, calsequestrin; SERCA2a, sarcoplasmic reticulum $Ca^{2+}$-ATPase; PLB, phospholamban; LVSP, LV systolic ejection pressure; HR, heart rate; ANOVA, analysis of variance; CICR, $Ca^{2+}$-induced $Ca^{2+}$ release; NS, statistically not significant; AR, adrenergic receptor; AC, adenylyl cyclase.

ity of S100A1 protein expression correlates with changes in cardiac contractile state. These data coupled with our findings that overexpressed S100A1 can increase myocyte contractile function *in vitro* indicate that this $Ca^{2+}$-binding protein may play an important role in myocardial regulation *in vivo*. Accordingly, in this study we have generated myocardial-targeted S100A1 overexpressing transgenic mice in order to determine the chronic *in vivo* physiological and morphological consequences of increased S100A1 expression in the heart.

## EXPERIMENTAL PROCEDURES

*Generation and Identification of Transgenic Mice*—Transgenic mice with a cardiac-specific overexpression of human S100A1 were created with the use of the murine α-myosin heavy chain gene promoter (13). The full-length human S100A1 cDNA (0.6 kb) was amplified by standard PCR techniques (6) and cloned into a previously described vector that contained the 5.5-kb α-myosin heavy chain promoter and a downstream simian virus 40 (SV40) intron poly(A) signal (0.7kB) (14). This construct (Fig. 1*A*) was linearized and purified before pronuclear injections were done by the Duke Comprehensive Cancer Center Transgenic Facility. Offspring were screened by Southern blot analysis with a probe for the SV40 sequence as described (14), and four distinct founder lines (S100A1-I to IV) were originally established. Litter sizes and development of transgenic animals were indistinguishable from those of nontransgenic littermate control (NLC) mice. Second-generation animals of the lines S100A1-I and -II both displayed the highest SV40 signals at the age of 5–8 months and were used for all studies in accordance with institutional guidelines.

*RNA Isolation and Northern Blot Analysis*—Total RNA was isolated by standard methods (14, 15) from S100A1 transgenic ventricles and NLC ventricles ($n$ = 3–5 each). 30 μg of total RNA was loaded and run on 1% formaldehyde gels and transferred to nitrocellulose. Hybridization was performed by standard techniques using radiolabeled cDNAs for S100A1, atrial natriuretic factor, and α-skeletal actin (14, 15). Blots were then stripped and reprobed with glyceraldehyde-3-phosphate dehydrogenase to control for RNA loading.

*Western Blotting*—Western blots were performed to assess cardiac protein levels of S100A1, dihydropyridine receptor $\alpha_2$-subunit ($\alpha_2$-DHPR, Advanced Biomedical Research, Inc.; MA3–921), ryanodine receptor (RyR2, Advanced Biomedical Research, Inc.; MA3–925), calsequestrin (CSQ, Calbiochem; 208915), sarcoplasmic reticulum $Ca^{2+}$-ATPase (SERCA2a, sc-8094), phospholamban (PLB, Upstate Biotechnology; 05–205), $Na^+/Ca^{2+}$ exchanger (Advanced Biomedical Research, Inc.: MA3–926), β-ARs ($\beta_1$AR sc-568, $\beta_2$AR sc-570), cardiac adenylyl cyclases (AC V/VI sc-590), PKA catalytic and regulatory subunit (PKA cat/reg sc-903/909), and serine 16-phosphorylated PLB (Upstate Biotechnology; 07–052) in NLC and TGS100A1 LV tissue using both soluble (supernatant) and membrane fractions as described (6, 16). To detect S100A1 protein levels in supernatant, we used a custom rabbit polyclonal antibody raised against human S100A1 protein (amino acids 42–54, anti-S100A1, SA 5632), which is cross-reactive for human, rabbit, rat, and mouse S100A1 protein as described (6).

*Assessment of $\alpha_1$-DHPR*—Cardiac membrane preparations (10-μg each) from TGS100A1 and control mice were incubated with 30 nM DM-BODIPY-dihydropyridine (Molecular Probes D-7443) (17) for 60 min at room temperature in equilibration buffer composed of 20 mM HEPES, pH 7.0, 150 mM NaCl, 1 mM EDTA, and 0.5% Tween 20. Samples were centrifuged at 100,000 × $g$ for 20 min, washed three times with equilibration buffer, and resuspended in 1 ml of the buffer. Fluorescence intensity of bound DM-BODIPY-dihydropyridine at 511 nm was measured with a PerkinElmer LS-50 luminescence spectrophotometer and used as a direct estimation of the DHPR $\alpha_1$-subunit content.

*Transthoracic Echocardiography*—Two-dimensional guided M-mode and Doppler echocardiography was carried out using an HDI 5000 echocardiograph (ATL, Bothell, WA) in conscious mice as previously described (18). Three independent echocardiographic measurements were taken in both modes. Left ventricular chamber diameter in end-systole (LVESD) and end-diastole (LVEDD), interventricular septum (IVSth), LV posterior (LVPth) wall thickness in end-diastole, and LV fractional shortening (FS%) were determined in a short-axis M-mode view at the level of the papillary muscles; FS% = LVEDD − LVESD/LVEDD × 100; (%). LV ejection time (LVET) and heart rate (bpm) taken from aortic valve Doppler measurements were used to assess heart rate corrected mean velocity of circumferential fiber shortening: mean Vcfc = FS%/ET × $\sqrt{}$60/bpm × 10; (circ/s).

*Cardiac Catheterization and Hemodynamic Assessment*—Closed-chest cardiac catheterization in the same mice that were used for echocardiographic measurements was performed as described previously (18). Hemodynamic analysis included heart rate (beats/min), maximal LV systolic ejection (LVSP), end-diastolic pressure, and maximal (LV $dP/dt_{max}$) and minimal (LV $dp/dt_{min}$) first derivate of LV pressure.

*Preparation of Adult Ventricular Cardiac Myocytes*—$Ca^{2+}$-tolerant ventricular myocytes from mouse hearts were isolated using a modified collagenase/protease method as previously published (19). Cardiac myocytes were plated with a density of 15,000 cells/cm$^2$ on laminin-coated dishes, stored at 37 °C, 95% $O_2$/5% $CO_2$, and used for experiments up to 4–8 h after isolation.

*Calibration and Measurement of $Ca^{2+}$ Transients and SR $Ca^{2+}$ Load in Cardiomyocytes*—Intracellular $Ca^{2+}$ transients of mouse ventricular cardiomyocytes were calibrated and measured as previously described (7). Briefly, isolated cells were washed in HEPES-modified medium 199 (M199) (Sigma), incubated in 1 ml of M199 (2 mM $[Ca^{2+}]_e$) with 2 μM Fura2-AM for 20 min at room temperature. Calibration and fluorescence measurements were carried out using an inverse Olympus microscope (I×70) with a UV filter connected to a monochromator (Polychrome II, T.I.L.L. Photonics GmbH, Germany). Cells were electrically stimulated with 1 Hz and excited at 340/380 nm. Fluorescence emission was detected at 510 nm, digitized, and analyzed with T.I.L.L.VISION software (v. 3.3). Baseline data from five consecutive steady-state transients were averaged for analysis of transient amplitude ($Ca^{2+}$ amplitude; (nM)), time to peak (ms), and time to 50% decline (ms). Calibration for Fura2-AM loaded mouse ventricular myocytes on 50 cells yielded a minimal ratio ($R_{min}$) of 0.38 ± 0.05 and a maximal ratio ($R_{max}$) of 3.36 ± 0.21, whereas $\beta$ and $K_d$ were estimated to amount to 5.21 ± 0.24 and 236 ± 29 nM, respectively. Free intracellular $Ca^{2+}$ concentration $[Ca^{2+}]_i$ was calculated by the equation of Grynkiewicz *et al.* (20): $[Ca^{2+}]_i = K_d \times \beta(R - R_{min})/(R_{max} - R)$. $Ca^{2+}$ transients were investigated at baseline and throughout a stepwise increase of isoproterenol concentrations ($10^{-9}$-$10^{-5}$ M) under electrical stimulation at 1 Hz and 2 mM $[Ca^{2+}]_e$ in M199. SR $Ca^{2+}$ load was assessed using a standard caffeine pulse protocol (21, 22). After 2 min of electrical stimulation (1 Hz), myocytes were abruptly exposed to 0 $Na^+$/0 $Ca^{2+}$ solution with caffeine (10 mM). The peak of the caffeine-induced $Ca^{2+}$ transient was used as an index of the SR $Ca^{2+}$ load.

*Myocyte Contractile Parameters*—Contractility studies of isolated ventricular myocytes were performed as recently described (6) with a video-edge detection system (Crescent Electronics, Sandy, UT). In brief, myocytes were electrically stimulated to contract at 1 Hz in M199 at room temperature; edge detection measurements were obtained under basal condition and incremental isoproterenol concentrations ($10^{-9}$-$10^{-5}$ M). Data from five consecutive steady-state twitches were averaged for analysis of fractional cellular shortening (%CS (%)), shortening velocity (-dL/dt, (μm/s)) and relengthening velocity (+dL/dt, (μm/s)).

*Preparation of Cardiac SR Vesicles*—Cardiac SR vesicle preparations from murine myocardium both from NLC and TG S100A1 hearts were carried out as described elsewhere (23).

*Co-immunoprecipitations*—Co-immunoprecipitation was carried out as previously described (24), with minor modifications, to investigate S100A1 protein interaction with RyR2, SERCA2a, and PLB. Murine SR cardiac membrane preparations from both TGS100A1 and NLC hearts (1 mg/ml protein) in 0.25 M sucrose, 10 mM Tris-HCl, pH 7.5, 20 μM $CaCl_2$, 150 mM KCl were mixed with an equal volume of 40 mM HEPES-NaOH, pH 7.5, 300 mM NaCl, 0.5 mM EDTA, 4 mM phenylmethylsulfonyl fluoride, 1% Tween 20. Suspensions were rotated with bovine serum albumin-treated A/G-Sepharose for 30 min and centrifuged to remove proteins bound nonspecifically to A/G-Sepharose. The supernatants were then mixed with A/G-Sepharose and precipitating antibodies either for RyR2 (RDI-RYANRabm), SERCA2a (sc-8094), PLB (Upstate Biotechnology; 05–205) or CSQ (Calbiochem; 208915). The samples were rotated for 30 min and centrifuged (800 × $g$), and pellets were washed three times with a buffer composed of 20 mM HEPES, pH 7.5, 20 μM $CaCl_2$, 150 mM NaCl, 0.5 mM EDTA, and 0.5% Tween 20. Samples were resolved by 4–20% SDS-PAGE, transferred to a polyvinylidene difluoride membrane, and stained for S100A1 (SA 5632).

*Assessment of $Ca^{2+}$-induced $Ca^{2+}$ Release (CICR) from Cardiac SR Vesicles*—SR $Ca^{2+}$ release from isolated SR vesicles from both NLC and TG S100A1 hearts was assessed by determining rapid $^{45}Ca^{2+}$ efflux with the Millipore filtration technique from passively preloaded SR vesicles as previously described (25, 26).

*β-AR and PKA Signaling Studies*—β-AR binding on crude membrane preparations (15 μg) from either TG S100A1 or NLC mice was performed by using the non-selective β-AR ligand [$^{125}$I]cyanopindolol as

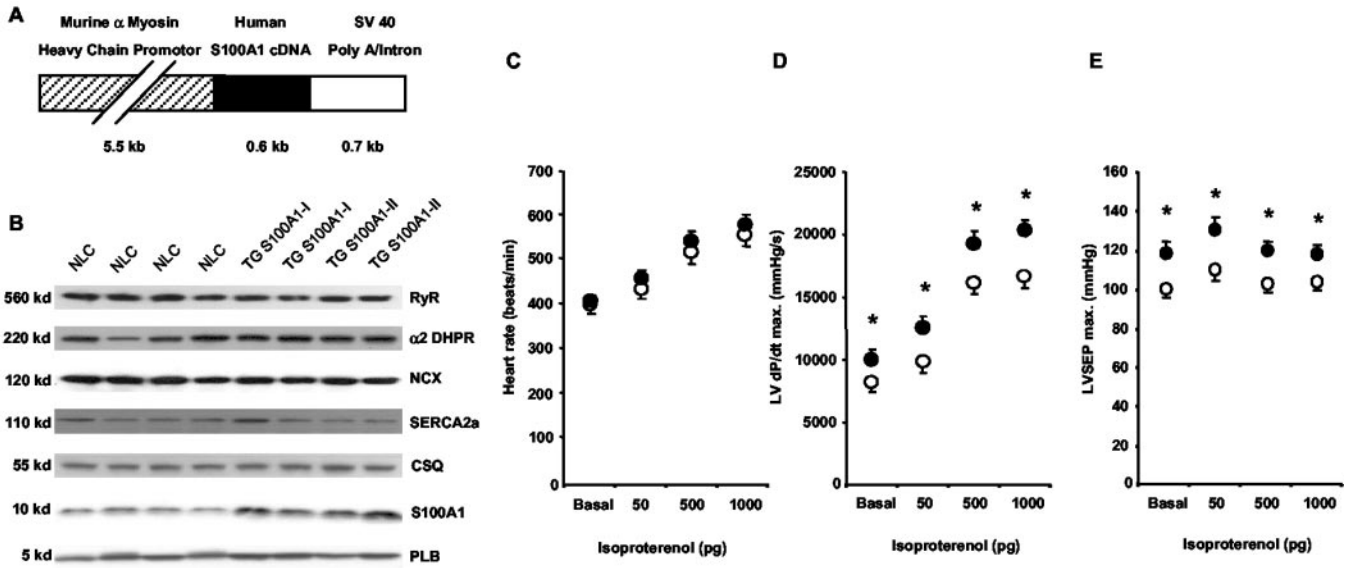


FIG. 1. **Characterization of TG S100A1 mice.** *A*, schematic depiction of the DNA construct used for generation of S100A1-overexpressing transgenic mice. *SV40*, simian virus 40. *B*, representative Western blot analysis for S100A1 and major cardiac $Ca^{2+}$ cycling proteins from LV mouse homogenates or membrane preparations of two animals each from TG S100A1-I and -II lines compared with their non-transgenic litter mate control (*NLC*) mice ($n = 6$). For abbreviations used, see "Experimental Procedures." Protein expression was normalized to calsequestrin (*CSQ*) levels; the relative mass is shown on the *left* in kilodaltons (*kD*). *C–E*, *in vivo* assessment of LV function at baseline (*basal*) and in response to progressive doses of the β-AR agonist isoproterenol in closed-chest anesthetized animals (○, NLC, $n = 18$; ●, TG S100A1 line I and II, $n = 18$). Shown are the *in vivo* responses for heart rate (*HR, beats/min*) (*C*), maximal first derivative of LV pressure rise ($LV\ dP/dt_{max}$) (*D*), maximal LV systolic ejection pressure (*LVSP*) (*E*). Data are means ± S.E. *, $p < 0.05$ *versus* NLC (ANOVA and Student's *t* test).

described (14). Nonspecific binding was determined in the presence of 20 μM alprenolol. For membrane AC activity, aliquots of these membranes were incubated for 15 min at 37 °C with [α-$^{32}$P]ATP under basal conditions or in the presence of $10^{-4}$ M isoproterenol, $10^{-2}$ M NaF, $10^{-4}$ M forskolin, and 2 mM $CaCl_2$; cAMP was quantitated as described (15). For PKA studies, mouse hearts were excised and perfused for 15 min with M199 to wash out endogenous catecholamines (unstimulated group); the β-AR-stimulated group was incubated for 3 min with $10^{-6}$ M isoproterenol. Hearts were snap-frozen in liquid $N_2$, and γ-$^{32}$P incorporation in heart extracts was determined and analyzed as described (27).

*Statistics*—Data are generally expressed as mean ± S.E. An unpaired Student's *t* test and two-way repeated measures ANOVA were performed for statistical comparisons. For all tests, a *p* value of <0.05 was considered as significant.

## RESULTS

*Generation and Characterization of S100A1 Transgenic Mice*—To investigate the physiological role of S100A1 *in vivo*, we generated transgenic mice with cardiac-restricted overexpression of the human S100A1 protein under the control of the murine α-myosin heavy chain promoter (Fig. 1*A*). Two independent lines (designated TG S100A1-I and TG S100A1-II) with nearly identical SV40 signals were identified by Southern and Northern blot analysis and used in parallel throughout the study to exclude an influence of positional effects of transgene integration. Myocardial S100A1 protein levels were determined in TG S100A1 and NLC mice. There was a similar ~4-fold significant increase of myocardial S100A1 protein levels in both TG S100A1-I and -II animals compared with NLCs (TG S100A1-I, 4.2 ± 0.9-fold *versus* NLC, $p < 0.01$, $n = 6$; TG S100A1-II, 3.8 ± 0.8-fold *versus* NLC, $p < 0.01$, $n = 6$; increase in S100A1 protein for TG S100A1-I *versus* TG S100A1-II, $p$ = NS, $n = 6$) (Fig. 1*B*). Compared with NLC mice, TG S100A1 mice had normal litter sizes; overall, these transgenic mice were grossly indistinguishable and had no increased morbidity or mortality. This included the finding that adult TG S100A1 animals >6 months of age had no cardiac pathology present, including normal cardiac mass. Biometric measurements are found in Table I. Consistent with the lack of cardiac hypertrophy following chronic myocardial S100A1 overexpression, we found no changes in ventricular mRNA expression of atrial natriuretic factor or α-skeletal actin, two molecular markers of hypertrophy, in TGS100A1 hearts compared with NLC (data not shown).

Because S100A1 can interact with several $Ca^{2+}$-regulating proteins such as RyR1 in skeletal muscle (28), we investigated the influence of chronic cardiac S100A1 overexpression on levels of major intracellular $Ca^{2+}$ cycling proteins. Fig. 1*B* displays representative protein expression results ($n = 6$) for cardiac RyR (RyR2), $\alpha_2$-DHPR, $Na^+/Ca^{2+}$ exchanger, SERCA2a, CSQ, and PLB (see "Experimental Procedures"). The levels of these proteins were compared in cardiac extracts (cytosolic or membrane preparations) prepared from TG S100A1 and NLC mice. We found no difference in the levels of these proteins in TG S100A1 mice when compared with NLCs (Fig. 1*B*). In addition to the $\alpha_2$-DHPR, levels of the $\alpha_1$-DHPR subunit, which is the major channel protein of the L-type voltage-dependent calcium channel, were assessed in TG S100A1 and NLC sarcolemmal membrane preparations by quantification of fluorescence DM-BODIPY-dihydropyridine binding (17). This revealed no significant difference between the groups (TG S100A1, 0.30 ± 0.03 *versus* NLC, 0.31 ± 0.06; $n = 6$; $p$ = NS. Data are given as relative fluorescence units).

*Hemodynamic Parameters in S100A1 Overexpressing Transgenic Mice*—To determine the *in vivo* functional consequences of myocardial-targeted S100A1 overexpression, cardiac catheterization was performed in closed-chest anesthetized animals. Hemodynamic measurements were recorded under basal conditions and after β-AR stimulation with isoproterenol as described (18). As shown in Table I, TG S100A1 mice exhibited a marked increase in basal cardiac function compared with NLC animals. TG S100A1 mice showed significantly higher LVSP accompanied by a significant increase in the first derivative of LV systolic pressure rise ($LV\ dP/dt_{max}$) and decline ($LV\ dP/dt_{min}$) compared with NLCs (Table I), demonstrating enhanced contractility and relaxation, respectively. Importantly, both heart rate (HR) and LV end diastolic pressure, parameters that can affect LV contractility, were indistinguishable in TG S100A1 and NLCs (Table I).

TABLE I
*Physiological and basal hemodynamic parameters in S100A1 transgenic mice*

NS, statistically not significant ($p > 0.05$); NLC, non-transgenic litter mate control mice; TG S100A1, S100A1 transgenic mice (lines I and II); LVSP, maximal left ventricular systolic ejection pressure; LVEDP, left ventricular end diastolic pressure. All data are presented as mean ± S.E.

| | NLC ($n$ = 18) | TG S100A1 ($n$ = 18) | $p$ value[a] |
|---|---|---|---|
| Body weight (g) | 29.77 ± 1.42 | 29.30 ± 1.80 | NS |
| Heart weight (mg) | 133.08 ± 5.56 | 128.53 ± 6.87 | NS |
| Heart/body ratio (mg/g) | 4.52 ± 0.13 | 4.46 ± 0.15 | NS |
| Lung weight (mg) | 192.38 ± 6.66 | 182.63 ± 3.55 | NS |
| Liver weight (g) | 1.41 ± 0.13 | 1.21 ± 0.21 | NS |
| Tibia length (mm) | 17.92 ± 0.16 | 17.86 ± 0.15 | NS |
| LVSP (mmHg) | 100 ± 4.15 | 118 ± 6.44 | <0.03 |
| LV $dP/dt_{max}$ (mm Hg/s) | 7749 ± 335 | 10274 ± 538 | <0.001 |
| LV $dP/dt_{min}$ (mm Hg/s) | −6936 ± 328 | −9438 ± 809 | <0.01 |
| LVEDP (mm Hg) | 6.45 ± 0.56 | 6.91 ± 1.14 | NS |
| Heart rate (HR, beats/min) | 399 ± 20.6 | 406 ± 13.8 | NS |

[a] Compared by paired $t$-test or ANOVA.

Interestingly, when TG S100A1 and NLC mice were challenged with isoproterenol, *in vivo* ventricular performance was significantly enhanced with cardiac S100A1 overexpression. This increased sensitivity to β-AR stimulation was seen with LV $dP/dt_{max}$ (Fig. 1*D*), LVSP (Fig. 1*E*), and LV $dP/dt_{min}$ (data not shown). HR responses to isoproterenol were identical in TG S100A1 and NLC mice (Fig. 1*C*).

*Echocardiographic Function of S100A1 Transgenic Mice*—To further investigate the effect of myocardial-targeted S100A1 overexpression on the morphological and functional cardiac phenotype, LV chamber dimensions, wall thickness, and contractile parameters were estimated by echocardiography in conscious TG S100A1 and NLC mice as described (18). These results are summarized in Table II. LV diameter at end-diastole as well as interventricular septum and LV posterior wall thickness were similar in TG S100A1 and NLC animals. However, LV chamber diameter in end-systole was found to be significantly reduced in TG S100A1 animals (Table II). Moreover, LV systolic ejection time was significantly reduced in S100A1 overexpressing mice, whereas HR again did not differ between groups. Accordingly, calculated values for LV fractional shortening and HR corrected mean Vcfc were significantly higher in TG S100A1 mice compared with NLC mice (Table II), indicating enhanced global cardiac function when myocardial levels of S100A1 are increased.

*Contractile Properties and $Ca^{2+}$ Handling of Isolated TG S100A1 Ventricular Myocytes*—To determine whether changes in cellular $Ca^{2+}$ cycling account for increased cardiac contractile function in TG S100A1 mice, contractile performance and intracellular $Ca^{2+}$ handling were examined in isolated ventricular myocytes from TG S100A1 mice and compared with measurements in NLC myocytes. Contractile properties of cardiac myocytes were assessed by the use of edge detection. Fig. 2*A* shows superimposed representative contractions taken from isolated S100A1 overexpressing and NLC myocytes. Although no significant difference in maximal diastolic length ($L_{max}$) occurred, isolated cardiac myocytes from TG S100A1 mice clearly exhibited a significant increase in cellular shortening that was accompanied by a significant increase of shortening and relengthening velocity, respectively (Table III). Thus, cardiac S100A1 overexpression causes a marked increase in cellular contractility, which is consistent with the above-described basal *in vivo* physiological data.

Because $Ca^{2+}$ signaling plays a central role in cardiac contractility, we assessed the influence of transgenic S100A1 overexpression on intracellular $Ca^{2+}$ handling. To visualize intracellular $Ca^{2+}$ kinetics, isolated cardiac myocytes were loaded with Fura2-AM and emission transients were recorded. Considering the non-linearity of the Fura2-ratio emission signal (20), $Ca^{2+}$ calibration in cardiac myocytes was performed with consistent values to previously published results (21, 22), whereas quenching revealed no significant dye compartmentalization because of our loading protocol (data not shown). Fig. 2*C* displays superimposed representative intracellular $Ca^{2+}$ transients obtained from TG S100A1 and NLC cardiac myocytes. Although diastolic $Ca^{2+}$ levels, time to peak, and time to 50% decline did not differ between both groups, the systolic rise of intracellular $Ca^{2+}$ levels was significantly higher in S100A1 overexpressing cardiac myocytes (Table III).

To elucidate the functional consequences of β-AR stimulation on TG S100A1 and NLC myocytes, measurements for cellular shortening and $Ca^{2+}$ transient amplitudes were carried out in response to increasing concentrations of isoproterenol. Fig. 2*B* depicts the increase in cell shortening in response to incremental β-AR stimulation in S100A1 overexpressing and NLC cardiac myocytes. Consistent with our *in vivo* findings, cardiac myocytes isolated from TG S100A1 mice responded with significantly higher contractility throughout all concentrations of isoproterenol. However, the relative increase in cell shortening did not differ significantly between both groups, demonstrating no change in β-AR responsiveness (data not shown). Because the inotropic effect of β-AR stimulation is ultimately based on enhancement of cytosolic $Ca^{2+}$ kinetics, we investigated whether S100A1 overexpression would also influence cellular $Ca^{2+}$ cycling following isoproterenol. Fig. 2*C* illustrates the effect of β-AR stimulation on intracellular $Ca^{2+}$ transient amplitudes in both S100A1 overexpressing and NLC cardiac myocytes. We also observed an enhancement in $Ca^{2+}$ transient amplitudes after administration of isoproterenol for cardiac myocytes from both TG S100A1 and NLC mice. Importantly, the S100A1-mediated increase in $Ca^{2+}$ transient amplitudes seen under basal conditions was maintained after β-AR stimulation because TG S100A1 myocytes had the highest $Ca^{2+}$ transients (Fig. 2*D*). As above, the relative increase in $Ca^{2+}$ transient amplitudes after isoproterenol was not significantly different in both groups (data not shown).

*Effect of S100A1 on SR $Ca^{2+}$ Load and $Ca^{2+}$-induced $Ca^{2+}$ Release*—To investigate the underlying mechanism for the increase in cytosolic $Ca^{2+}$ transients, we assessed SR $Ca^{2+}$ load under basal conditions and in response to β-AR stimulation in isolated cardiomyocytes isolated from TG S100A1 and NLC mice ($n$ = 30 from 3 different animals each). Fig. 3*A* displays superimposed representative caffeine-induced $Ca^{2+}$ transients obtained from a TG S100A1 and NLC myocyte under basal conditions where TG S100A1 myocytes have enhanced transients. The overall SR $Ca^{2+}$ load was significantly higher in TG S100A1 myocytes under basal conditions and after the addition of isoproterenol (Fig. 3*B*). Because S100A1 has been shown both to interact with the skeletal muscle RyR1 (28) and to enhance SR $Ca^{2+}$ release from skeletal muscle fibers (29), we

TABLE II

*In vivo echocardiographic assessment of cardiac properties of S100A1 transgenic mice*

All data are presented as mean ± S.E. NS, statistically not significant ($p > 0.05$); NLC, non-transgenic litter mate control mice; TG S100A1, S100A1 transgenic mice (line I and II); LVEED, left ventricular end diastolic diameter; IVSth, interventricular septal wall thickness; LVPWth, left ventricular posterior wall thickness; LVESD, left ventricular end systolic diameter; LVET, left ventricular ejection time; FS, fractional shortening; mean Vcfc, heart rate corrected mean velocity of circumferential fiber shortening.

| | NLC ($n$ = 18) | TG S100A1 ($n$ = 18) | $p$ value[a] |
|---|---|---|---|
| LVEDD (mm) | 3.26 ± 0.11 | 3.10 ± 0.10 | NS |
| IVSth (mm) | 0.77 ± 0.04 | 0.80 ± 0.03 | NS |
| LVPWth (mm) | 0.70 ± 0.04 | 0.73 ± 0.03 | NS |
| LVESD (mm) | 1.22 ± 0.06 | 1.00 ± 0.05 | <0.03 |
| LVET (ms) | 42.06 ± 1.81 | 35.09 ± 1.22 | <0.01 |
| Heart rate (beats/min) | 719 ± 30 | 664 ± 16 | NS |
| FS (%) | 60.8 ± 0.78 | 68.3 ± 0.42 | <0.01 |
| Mean Vcfc (circ/sec) | 4.37 ± 0.14 | 5.96 ± 0.10 | <0.01 |

[a] Compared by paired $t$-test or ANOVA.

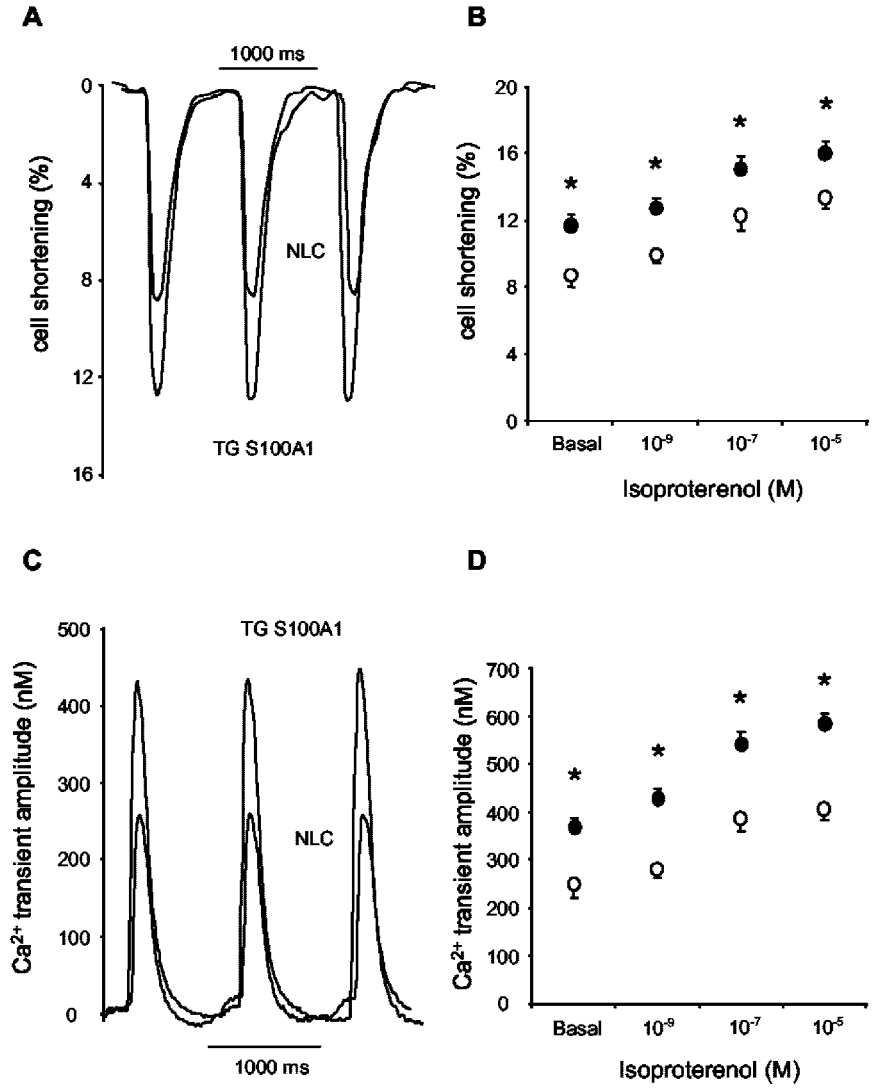


FIG. 2. **Effect of S100A1 on basal and β-adrenergic-stimulated contractility and $Ca^{2+}$ transients in isolated cardiomyocytes.** *A* and *C*, original superimposed tracings of cell shortening (%, shown as downward deflection, *left upper panel*) and intracellular $Ca^{2+}$ transients (nM, shown as upward deflection, *left lower panel*) under basal conditions (1 Hz, 2 mM $[Ca^{2+}]_e$) from representative TG S100A1- and NLC-isolated cardiac myocytes, respectively. *B* and *D*, increase of cell shortening (%, *panel B*) and $Ca^{2+}$ transient amplitudes (nM, *panel D*) in response to isoproterenol (given in molar). (○, NLC cardiac myocytes, $n$ = 100; ●, TG S100A1 cardiac myocytes, $n$ = 100). Three hearts from each TG S100A1 line (I and II) (6 total TG S100A1) were examined, and 15–20 cardiac myocytes from each heart were studied (see "Experimental Procedures"). Data shown are mean ± S.E. *, $p < 0.05$ *versus* NLC cardiac myocytes (ANOVA and Student's $t$ test).

investigated the effect of S100A1 on CICR from cardiac TG S100A1 and NLC SR vesicle preparations. CICR was assessed from passively $Ca^{2+}$-loaded SR vesicles using $^{45}Ca^{2+}$ as a radioactive tracer to quantify SR $Ca^{2+}$ efflux. SR vesicles derived from TG S100A1 hearts displayed a significantly time-dependent enhancement of CICR (Fig. 3*D*) that coincides with a 2.1 ± 0.3-fold ($p < 0.05$, $n$ = 3) higher amount of S100A1 protein found in TG S100A1 SR vesicles compared with NLC (Fig. 3*C*, *upper panel*). To assess whether this effect was specifically because of S100A1 protein, TG S100A1 and NLC SR vesicles were incubated with 2 mM EGTA for 30 min, followed by several washings steps in EGTA-free storage buffer to remove the $Ca^{2+}$ chelating compound. EGTA treatment apparently led to S100A1 depletion of SR membranes (Fig. 3*C*, *upper panel*), resulting in diminished SR $Ca^{2+}$ release in both groups and a complete loss of the S100A1-mediated gain in CICR in TG S100A1 SR vesicles (Fig. 3*D*). To determine a potential molecular mechanism for increased SR $Ca^{2+}$ load and release, we carried out co-immunoprecipitations for S100A1 with either SERCA2a, PLB, or cardiac RyR2. These experiments revealed no evidence for a direct interaction of S100A1 with the SERCA2a·PLB complex (data not shown). However, under con-

TABLE III
*Basal contractile properties and calcium transients of S100A1 transgenic cardiac myocytes*

NS, statistically not significant ($p > 0.05$); NLC, non-transgenic litter mate control; TG S100A1, S100A1 transgenic mice (lines I and II); % CS; % cell shortening; $L_{max}$, maximal cardiac myocyte length; −dL/dt, rate of cell shortening; +dL/dt, rate of cell re-lengthening; $\Delta[Ca^{2+}]_i$, calcium transient amplitude; diastolic $[Ca^{2+}]_i$, diastolic intracellular calcium levels; TTPn, normalized time to peak; T50n, normalized time to 50% decline. All data are presented as mean ± S.E. and were pooled from 100 cells from 6 different animals per group.

| | NLC ($n$ = 100) | TG S100A1 ($n$ = 100) | $p$ value[a] |
|---|---|---|---|
| Contractile properties | | | |
| % CS (%) | 8.42 ± 0.41 | 12.02 ± 0.33 | <0.01 |
| $L_{max}$ ($\mu$m) | 126 ± 9 | 128 ± 7 | NS |
| −dL/dt ($\mu$m/s) | 190 ± 9 | 294 ± 13 | <0.01 |
| +dL/dt ($\mu$m/s) | 110 ± 10 | 212 ± 8 | <0.01 |
| Calcium transients | | | |
| $\Delta[Ca^{2+}]_i$ (nM) | 255 ± 17 | 342 ± 22 | <0.01 |
| Diastolic $[Ca^{2+}]_i$ (nM) | 133 ± 17 | 142 ± 28 | NS |
| TTPn (ms) | 124 ± 13 | 135 ± 22 | NS |
| T50n (ms) | 218 ± 17 | 187 ± 23 | NS |

[a] Compared by Student's $t$ test.

ditions where S100A1 does not interact with SERCA2A and PLB, S100A1 protein was found, for the first time, to interact with RyR2 (Fig. 3*C*, *lower panel*). This interaction was not found in EGTA-S100A1 depleting condition (Fig. 3*C*, *lower panel*). This interaction between S100A1 and RyR2 occurs in NLC mice, but increased S100A1 was co-immunoprecipitated in TG S100A1 hearts, indicating a specific association (Fig. 3*C*, *lower panel*). Thus, the S100A1-mediated increase in cytosolic $Ca^{2+}$ cycling seems at least caused by both augmented CICR and SR $Ca^{2+}$ load, presumably through a direct S100A1-RyR2 interaction or potentially through an indirect mechanism on SERCA2a/PLB.

*Effect of S100A1 Overexpression on Cardiac β-AR Signaling*—To explore whether the phenotype of enhanced cardiac function in TG S100A1 mice was because of alterations of the cardiac β-AR-AC-PKA pathway, we analyzed the levels of associated proteins, including β-AR density and AC activity in membranes isolated from TG S100A1 and NLC mice. As shown in Fig. 4*A*, cardiac S100A1 overexpression did not alter the protein levels of any these signaling molecules, including $\beta_1$- and $\beta_2$-ARs, AC, and PKA. Radioligand binding also showed that myocardial total β-AR density did not differ between TG S100A1 (40.12 ± 3.57 fmol/mg protein) and NLC (42.45 ± 1.71 fmol/mg protein, $p$ = NS, $n$ = 6 each) mice. S100A1 overexpression did not alter membrane AC activity either; Fig. 4*B* shows that basal as well as isoproterenol, NaF, and forskolin-stimulated cAMP generation was not altered in TG100A1 myocardial membranes compared with NLCs. Moreover, $Ca^{2+}$ inhibition of AC was similar (Fig. 4*B*). These data indicate that there is preserved β-AR coupling and unaltered enzymatic activity of AC in TG S100A1 hearts.

Finally, we examined several downstream targets of β-AR-mediated PKA in the myocardium; these were also unchanged in TG S100A1 hearts when compared with NLC mice. The basal PLB phosphorylation state as well as its relative increase in response to isoproterenol ($10^{-4}$ M) stimulation did not differ between TG S100A1 and control (Fig. 4*A*). Moreover, as shown in Fig. 4*C*, the phosphorylation states of PLB, troponin I, and myosin-binding protein C were indistinguishable between TG S100A1 and NLC hearts. This again was true for basal and isoproterenol-stimulated conditions.

## DISCUSSION

Because S100A1 has been shown to be up-regulated in compensated cardiac hypertrophy where normal contractile function is maintained (12) but is significantly down-regulated when the heart is failing (3, 8), we postulated that this molecule might be involved in the regulation of *in vivo* cardiac contractility. In the current study, we demonstrate for the first time that myocardial-targeted transgenic overexpression of S100A1 leads to a marked improvement of *in vivo* cardiac function in mice both under baseline conditions and in response to β-AR stimulation. Cardiomyocyte SR $Ca^{2+}$ cycling is also enhanced after transgenic cardiac S100A1 overexpression, contributing to increased *in vivo* myocardial contractility. Further, in the current study, we have revealed the novel finding that S100A1 can associate with the cardiac RyR2 isoform and that this interaction may take part in its inotropic mechanism by enhancing SR $Ca^{2+}$ release.

In addition, within the time frame of this study (~7 months of age), a 4-fold overexpression of S100A1 in the hearts of mice did not lead to any detrimental effects on cardiac morphology or physiology. Although cardiac function was markedly increased in response to chronic S100A1 overexpression, both echocardiographic measurements and assessment of heart and ventricle weights demonstrated that hearts from TG S100A1 mice had relatively normal dimensions and mass compared with NLC hearts. In support of this, most recently it has been shown (8) that S100A1 gene addition to cardiomyocytes even inhibits activation of the atrial natriuretic factor and α-skeletal actin promoter in response to α-adrenergic hypertrophic stimuli *in vitro*. Consistent with these findings, there was no up-regulation of molecular markers of cardiac hypertrophy, such as atrial natriuretic factor and α-skeletal actin, in response to cardiac-restricted S100A1 gene addition *in vivo*. These results suggest that the increase in S100A1 expression found in cardiac hypertrophy (12) is a result of the compensation and not causative.

*In vivo* hemodynamic assessment by cardiac catheterization and echocardiography revealed that TG S100A1 mice have a phenotype of enhanced cardiac function. LV catheterization of anesthetized TG S100A1 mice demonstrated a marked increase both in systolic and diastolic cardiac function under baseline conditions as indicated by cardiac contractility (LVSP and LV $dP/dt_{max}$) and relaxation (LV $dP/dt_{min}$). Importantly, there were no observed differences in LV end-diastolic pressure or HR, all of which could contribute to the gain in cardiac function, indicating that there is indeed increased cardiac performance as the result of chronic myocardial overexpression of S100A1. The enhancement of *in vivo* cardiac performance seen under baseline conditions measured by resting echocardiography and cardiac catheterization also translated to an increased inotropic reserve because *in vivo* β-AR function was similarly enhanced after isoproterenol administration. Interestingly, β-adrenergic responsiveness, as measured by the relative difference between baseline contractile parameters and responses after maximum isoproterenol, did not differ in TG S100A1 mice compared with NLCs. Thus, S100A1 overexpression does not appear to enhance cardiac sensitivity for β-AR activation but rather can augment β-adrenergic signaling, possibly through alternative downstream events. In support of this, we found no difference in β-AR signaling in TG S100A1 mouse hearts as assessed by myocardial β-AR levels, cAMP generation, or PKA activity. This includes no change in the phosphorylation state of PLB, troponin I, or myosin-binding protein C.

To gain further insight into functional responses in S100A1-overexpressing myocardium, single-cell contractility was examined in isolated cardiac myocytes at rest and after stimulation with isoproterenol. S100A1 overexpression caused a marked increase in cellular shortening that was accompanied by a significant acceleration in the rate of myocyte shortening

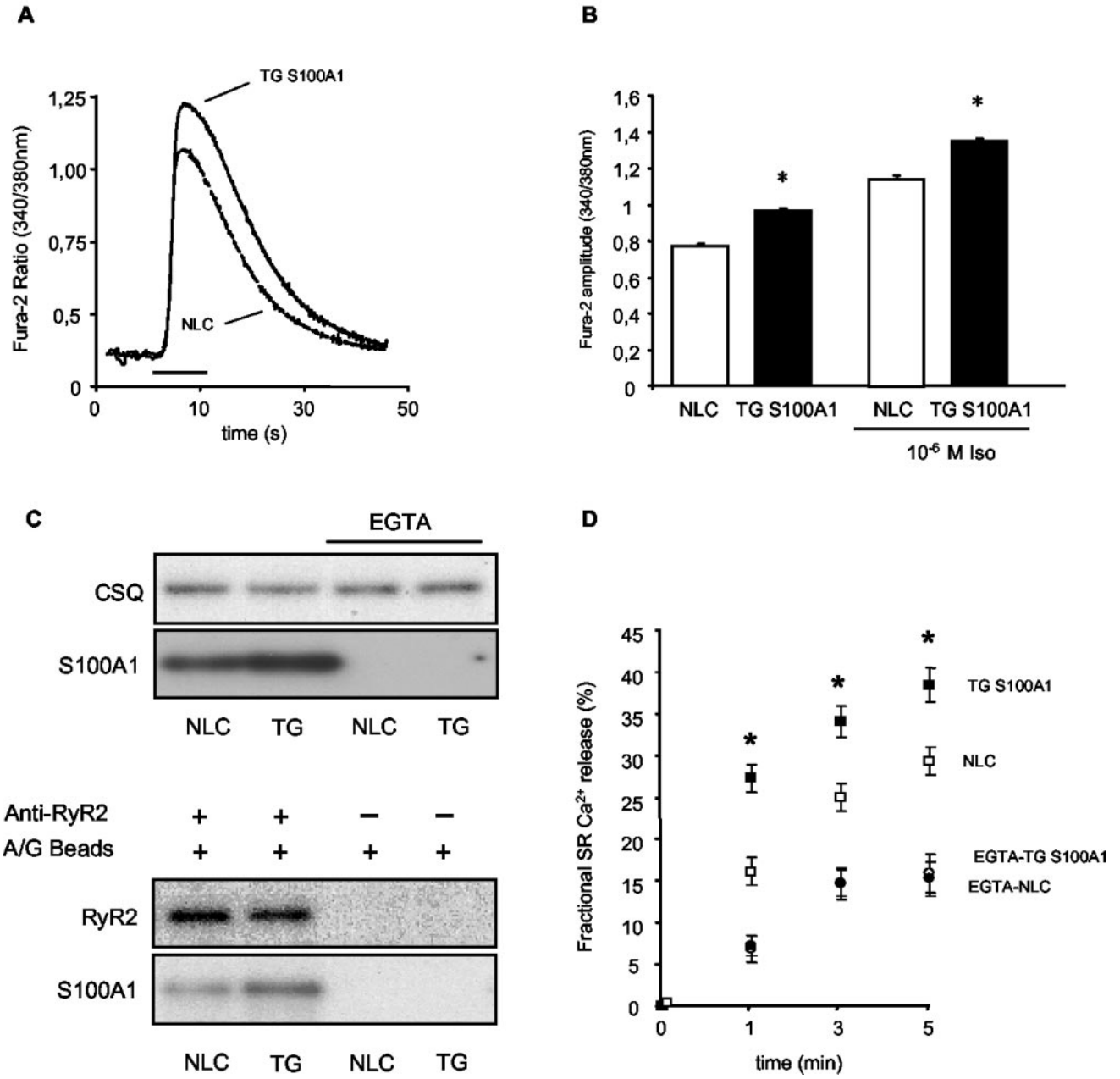


FIG. 3. **Effect of S100A1 protein on sarcoplasmic CICR.** *A* and *B*, effect of chronic S100A1 overexpression on SR $Ca^{2+}$ content assessed by caffeine application under basal conditions and isoproterenol stimulation. *A*, original superimposed tracings of caffeine-induced $Ca^{2+}$ transients obtained from representative TG S100A1 and NLC cardiac myocytes following electrical stimulation with 1 Hz and 2 mM $[Ca^{2+}]_e$. *B*, S100A1-mediated increase in SR $Ca^{2+}$ load estimated from the caffeine-induced $Ca^{2+}$ transient amplitude under basal and isoproterenol-stimulated conditions (NLC cardiac myocytes, $n = 30$; TG S100A1 cardiac myocytes, $n = 30$; cells were obtained from three different hearts per group). *, $p < 0.05$ *versus* NLC cardiac myocytes (ANOVA and Student's *t* test). *C*, representative Western blot analysis of S100A1 protein content in SR vesicles from NLC and TG S100A1 (*TG*) hearts (*upper panel*). Depletion of S100A1 protein because of EGTA treatment indicates $Ca^{2+}$-dependent association of S100A1 protein with SR proteins and membranes. Calsequestrin (*CSQ*) staining served as a control. Representative Western blot analysis for RyR2/S100A1 co-immunoprecipitation (*lower panel*). S100A1 appears to interact with the cardiac RyR isoform (*RyR2*) both in NLC and TG S100A1 membranes. Treatment of SR vesicles with A/G-Sepharose served as control. *D*, S100A1-mediated time-dependent increase in $Ca^{2+}$ induced $Ca^{2+}$ release from TG S100A1 cardiac SR vesicles (■) compared with NLC (□). S100A1-depletion of SR vesicles following EGTA treatment (*upper panel*) diminished CICR both in TG S100A1 (●) and NLC (○) SR membranes and completely abolished the gain in CICR in TG S100A1 SR vesicles (■) ($n = 6$, *, $p < 0.05$ *versus* NLC and EGTA-treated membranes) (ANOVA and Student's *t* test). Amount of CICR is given as fractional SR $Ca^{2+}$ release (%) from maximal SR vesicle $Ca^{2+}$ load. At the end of $Ca^{2+}$ uptake, vesicles contained 45 ± 6 nmol $Ca^{2+}$/0.1 mg protein.

and relengthening when compared with control cardiac myocytes from NLC mice. As found *in vivo*, there was no significant difference in the response to β-AR stimulation when measuring the relative increase in the contractile state in TG S100A1 and NLC cardiomyocytes. These data confirm that the functional improvement of S100A1 transgenic hearts seen *in vivo* appears to be based on an increase in contractility at the cellular level. Overall, the enhanced inotropic response seen to acute hemodynamic stress *in vivo* can be attributed to the enhanced baseline cardiac contractile enhancement in the cardiac myocyte and is possibly due to an extended intracellular release of contractile $Ca^{2+}$ by S100A1 following β-AR stimulation.

Because $Ca^{2+}$ is the key regulator of muscle contraction, alterations in protein levels of cardiac $Ca^{2+}$ cycling proteins, such as the cardiac DHPR, RyR2, $Na^+/Ca^{2+}$ exchanger, SERCA2, or PLB may also be involved in the increased cardiac

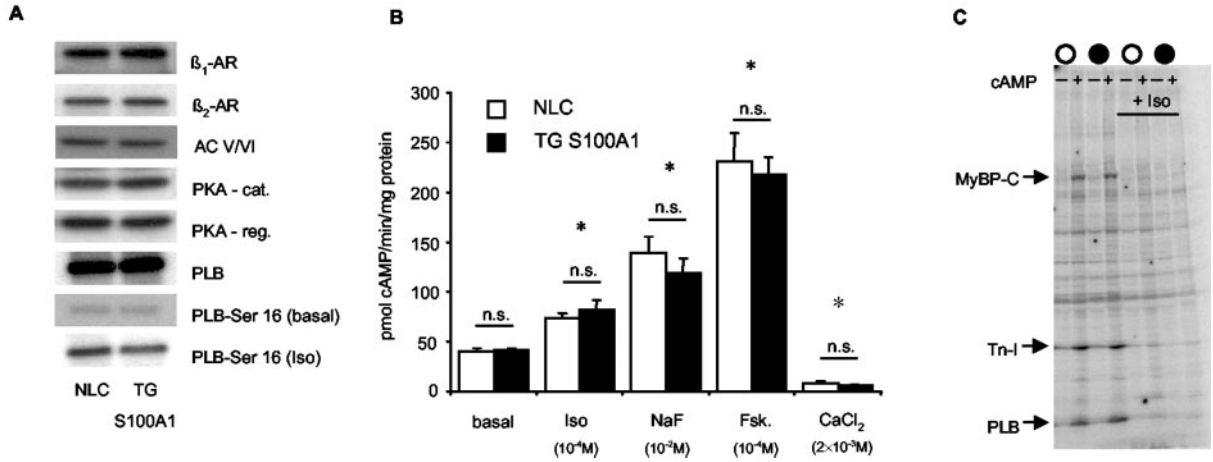


FIG. 4. **Effect of S100A1 overexpression on the cardiac β-AR signaling pathway.** *A*, representative Western blot analysis of β-adrenergic signaling components in membrane fractions or homogenized cellular preparations from TG S100A1 and NLC hearts ($n = 6$). For detection of $\beta_{1/2}$AR single bands, short exposure times (5–10 s) were chosen. For abbreviations used, see "Experimental Procedures." *B*, assessment of myocardial membrane AC activity (pmol cAMP/min/mg protein) in pooled membrane extracts from NLC ($n = 8$) and TG S100A1 hearts (lines I and II, $n = 4$ each) under basal conditions and in response to isoproterenol ($10^{-4}$ M), NaF ($10^{-2}$ M), forskolin ($10^{-4}$ M), and $CaCl_2$ ($2 \times 10^{-3}$ M). Measurements were performed in duplicate. *, $p < 0.05$ *versus* basal (ANOVA). *C*, autoradiograph of a representative back-phosphorylation assay from control and isoproterenol (*Iso*)-stimulated LV protein extracts from NLC (○) and TG S100A1 (●) hearts with (+) or without (−) cAMP addition. *Arrows* indicate the positions of non-phosphorylated (−) and back-phosphorylated (+) myosin-binding protein C (*MyBP-C*), troponin I, (*Tn-I*) and PLB.

contractility seen in TG S100A1 mice because changes in the expression and/or activity of these proteins can lead to alterations in cardiac function in mice (19, 30–33). Western blot analysis and quantitative fluorescent ligand binding excluded any change in protein levels or functional status (*i.e.* phosphorylated PLB) of these $Ca^{2+}$-interacting molecules, which is consistent with our recent finding of unaltered SERCA2a/PLB protein ratios after S100A1 gene transfer *in vitro* (6).

Previous observations *in vitro* demonstrated that increased levels of S100A1 protein enhance intracellular $Ca^{2+}$ cycling at least in part by an improved SR $Ca^{2+}$ uptake in saponin-skinned ventricular cardiomyocytes (6, 7). Thus, it was of interest to determine in these S100A1 transgenic mice whether the enhancement of *in vivo* cardiac function is also related to specific changes in intracellular $Ca^{2+}$ fluxes and SR $Ca^{2+}$ movements. Our functional analysis of intracellular $Ca^{2+}$ transients in isolated TG S100A1 cardiomyocytes indeed showed an enhancement in peak systolic $Ca^{2+}$ levels, whereas diastolic $Ca^{2+}$ concentrations, time to peak, and time to 50% decline remained unchanged. Importantly, assessment of SR $Ca^{2+}$ load in TG S100A1 myocytes both at rest and under β-AR stimulation indicates that the S100A1-mediated gain in contractility is partly caused by an enhancement in SR $Ca^{2+}$ content. Although S100A1 has been found to co-localize with the SR (34) and assumed to interact with SERCA (35), co-immunoprecipitation with TG S100A1 and NLC hearts so far revealed no evidence for a direct interaction of S100A1 with either SERCA2a or PLB. Thus, further studies will have to clarify whether S100A1 may directly affect cardiac SERCA activity or enhance SR $Ca^{2+}$ load by a SERCA2a-independent mechanism. However, because S100A1 has been shown to interact with the skeletal RyR1 (28), resulting in enhanced SR $Ca^{2+}$ release in murine skeletal muscle fibers (29), we found, for the first time, that S100A1 can interact with the murine cardiac RyR2 isoform. Importantly, this interaction was not seen in S100A1-depeleted SR membrane preparations. In line with these results, SR vesicles derived from TG S100A1 hearts containing a nearly 2-fold higher amount of S100A1 protein displayed enhanced fractional SR $Ca^{2+}$ release compared with NLC. Unchanged CICR both in S100A1-depleted SR vesicles from TG S100A1 and NLC hearts confirmed specificity of the S100A1-dependent increase in CICR. We therefore conclude that S100A1 augments cardiac intracellular $Ca^{2+}$ homeostasis at least partially by enhanced SR function via a RyR2 interaction.

Although there are previous *in vitro* reports that S100A1 can interact or modulate AC and PKA activity (36, 37), we found no alterations on activity of these enzymes in TG S100A1 hearts. This is consistent with previous data using adenoviral-mediated S100A1 overexpression in cardiomyocytes because the increase contractile function seen *in vitro* was cAMP-independent (6). S100A1-induced positive inotropy appears to be specific for this family member in the heart because other S100 proteins have not shown this characteristic. Indeed, transgenic mice with cardiac S100B overexpression did not have increased cardiac function (38). This is especially interesting because this protein shows both high homology in primary sequence and similarity in the three-dimensional structure with S100A1 (39, 40). These results suggest little functional redundancy among S100 proteins in the adult heart.

Importantly, the cardiac phenotype of S100A1 knockout mice has recently been reported as one of blunted cardiac inotropic and lusitropic response to β-AR stimulation (27). Interestingly, S100A1 knockout mice, like S100A1 transgenic mice, have normal β-AR chronotropic responses (27). Thus, manipulation of S100A1 expression in the heart *in vivo* has profound effects on β-AR-mediated cardiac function. However, this apparent reciprocal effect between S100A1 knockout and transgenic overexpression is limited to β-AR-mediated responses because cardiac S100A1 overexpression led to enhanced basal cardiac function, which was not altered in S100A1 knockout hearts (28). In fact, TG S100A1 mice do not have enhanced β-AR responsiveness, and the increased β-AR-mediated contractile effects appear to be because of the enhanced basal function.

Nonetheless, these results in S100A1 knockout and transgenic mice are compelling, especially when also taking into account that S100A1 is significantly down-regulated in end-stage human heart failure (3), a condition that is accompanied by severely impaired β-AR signaling (41). Although the total ablation of the S100A1 gene in mice resulted in the deterioration of contractile performance upon adaptive myocardial growth in response to transaortic constriction (TAC), heterozygous S100A1 knockout mice showed a dramatic up-regulation

of S100A1 protein to physiological levels after TAC that coincided with a significant increase in cardiac contractile performance indistinguishable from that seen in wild-type animals (27). Thus, S100A1 appears to play an important role in maintaining cardiac contractility and β-AR responsiveness in cardiomyocytes, and its loss or lowering of expression in the heart may contribute to dampened responsiveness seen in the hypertrophied and failing heart. From our SR and co-immunoprecipitation results, the role of S100A1 in cardiac inotropy may be through an interaction with RyR.

It will be critical to determine the ultimate pathophysiological relevance of S100A1 protein in the heart, which has been in question since the finding that this EF-hand $Ca^{2+}$-binding protein was found to be down-regulated in the failing human heart (3). Interestingly, numerous S100A1-interacting proteins have been described *in vitro* (*e.g.* AC, PKA, titin, and actin (for review see Ref. 5). However, these interactions appear not to be important for the *in vivo* actions of S100A1 in the murine heart. Concerning cardiac function, our novel results suggest that S100A1 overexpression causes an enhancement in myocardial contractility *in vivo* at least because of increased SR function resulting in enhanced cytosolic $Ca^{2+}$ homeostasis independent of cAMP-dependent signaling. Although we found no change in the levels of the L-type voltage-dependent calcium channel, the impact of S100A1 overexpression on sarcolemmal $Ca^{2+}$ handling in the adult myocardium remains elusive and will be the subject of further studies. Importantly, the development of genetically engineered *in vivo* models of cardiac S100A1 expression such as the mice in this study provides powerful models to use in future studies to further delineate the molecular mechanisms of the actions of S100A1 in the cardiomyocyte.

We strongly believe that our current *in vivo* results in transgenic mice showing enhanced cardiac function without hypertrophy or detrimental effects coupled with previous *in vitro* studies with adenoviral-mediated S100A1 gene transfer to myocytes provide novel evidence that positive manipulation of S100A1 expression levels in the heart may also prove to be beneficial in the treatment of heart failure. Importantly, it is now possible to test this hypothesis both in genetic murine models of cardiomyopathy and *in vivo* gene transfer to larger animal models of heart failure, and this will be the subject of future investigations.

*Acknowledgments*—We thank Emily A. Greene, Christopher Cooper, and Nora Tenis for excellent technical assistance.

REFERENCES


1. Clapham, D. E. (1995) *Cell* **80,** 259–268
2. Kato, K., Kimura, S., Haimoto, H., and Suzuki, F. (1986) *J. Neurochem* **46,** 1555–1560
3. Remppis, A., Greten, T., Schafer, B. W., Hunziker, P., Erne, P., Katus, H. A., and Heizmann, C. W. (1996) *Biochim. Biophys. Acta* **1313,** 253–257
4. Kato, K., and Kimura, S. (1985) *Biochim. Biophys. Acta* **842,** 146–150
5. Donato, R. (2001) *Int. J. Biochem. Cell Biol.* **33,** 637–668
6. Most, P., Bernotat, J., Ehlermann, P., Pleger, S. T., Reppel, M., Borries, M., Niroomand, F., Pieske, B., Janssen, P. M., Eschenhagen, T., Karczewski, P., Smith, G. L., Koch, W. J., Katus, H. A., and Remppis, A. (2001) *Proc. Natl. Acad. Sci. U. S. A.* **98,** 13889–13894
7. Remppis, A., Most, P., Löffler, E., Ehlermann, P., Bernotat, J., Pleger, S. T., Börries, M., Repper, M., Fischer, J., Koch, W. J., Smith, G. L., and Katus, H. A. (2002) *Basic Res. Cardiol.* **97,** I/56-I/62
8. Tsoporis, J. N., Marks, A., Zimmer, D. B., McMahon, C., and Parker, T. G. (2003) *Mol. Cell Biochem.* **242,** 27–33
9. Schwartz, A., Sordahl, L. A., Entman, M. L., Allen, J. C., Reddy, Y. S., Goldstein, M. A., Luchi, R. J., and Wyborny, L. E. (1973) *Am. J. Cardiol.* **32,** 407–422
10. Gwathmey, J. K., Copelas, L., MacKinnon, R., Schoen, F. J., Feldman, M. D., Grossman, W., and Morgan, J. P. (1987) *Circ. Res.* **61,** 70–76
11. Wolff, M. R., Buck, S. H., Stoker, S. W., Greaser, M. L., and Mentzer, R. M. (1996) *J. Clin. Investig.* **98,** 167–176
12. Ehlermann, P., Remppis, A., Guddat, O., Weimann, J., Schnabel, P. A., Motsch, J., Heizmann, C. W., and Katus, H. A. (2000) *Biochim. Biophys. Acta* **1500,** 249–255
13. Subramaniam, A., Jones, W. K., Gulick, J., Wert, S., Neumann, J., and Robbins, J. (1991) *J. Biol. Chem.* **266,** 24613–24620
14. Koch, W. J., Rockman, H. A., Samama, P., Hamilton, R. A., Bond, R. A., Milano, C. A., and Lefkowitz, R. J. (1995) *Science* **268,** 1350–1353
15. Iaccarino, G., Rockman, H. A., Shotwell, K. F., Tomhave, E. D., and Koch, W. J. (1998) *Am. J. Physiol.* **275,** H1298–1306
16. Ehlermann, P., Redweik, U., Blau, N., Heizmann, C. W., Katus, H. A., and Remppis, A. (2001) *Gen. Physiol. Biophys.* **20,** 203–207
17. Knaus, H. G., Moshammer, T., Friedrich, K., Kang, H. C., Haugland, R. P., and Glossman, H. (1992) *Proc. Natl. Acad. Sci. U. S. A.* **89,** 3586–3590
18. Kohout, T. A., Takaoka, H., McDonald, P. H., Perry, S. J., Mao, L., Lefkowitz, R. J., and Rockman, H. A. (2001) *Circulation* **104,** 2485–2491
19. Adachi-Akahane, S., Lu, L., Li, Z., Frank, J. S., Philipson, K. D., and Morad, M. (1997) *J. Gen. Physiol.* **109,** 717–729
20. Grynkiewicz, G., Poenie, M., and Tsien, R. Y. (1985) *J. Biol. Chem.* **260,** 3440–3450
21. Ito, K., Yan, X., Feng, X., Manning, W. J., Dillmann, W. H., and Lorrel, B. H. (2001) *Circ. Res.* **89,** 422–429
22. Lalli, M. J., Jong, J., Prasad, V., Hashimoto, K., Plank, D., Babu, G. J., Kirkpatrick, D., Walsh, R. A., Sussman, M., Yatani, A., Marban, E., and Periasamy, M. (2001) *Circ. Res.* **89,** 160–167
23. Saito, A., Seiler, S., Chu, A., and Fleischer, S. (1984) *J. Cell Biol.* **99,** 875–885
24. Asahi, M., McKenna, E., Kurzydlowski, K., Tada, M., and MacLennan, D. H. (2000) *J. Biol. Chem.* **275,** 15034–15038
25. Meissner, G., Darling, E., and Eveleth, J. (1986) *Biochemistry* **25,** 236–244
26. Rousseau, E., Smith, J. S., Henderson, J. S., and Meissner, G. (1986) *Biophys. J.* **50,** 1009–1014
27. Du, X. J., Cole, T. J., Tenis, N., Gao, X. M., Kontgen, F., Kemp, B. E., and Heierhorst, J. (2002) *Mol. Cell. Biol.* **22,** 2821–2829
28. Treves, S., Scutari, E., Robert, M., Groh, S., Ottolia, M., Prestipino, G., Ronjat, M., and Zorzato, F. (1997) *Biochemistry* **36,** 11496–11503
29. Most, P., Remppis, A., Weber, C., Bernotat, J., Ehlermann, P., Pleger, S. T., Kirsch, W., Weber, M., Uttenweiler, D., Smith, G. L., Katus, H. A., and Fink, R. H. (2003) *J. Biol. Chem.* **278,** 26356–26364
30. Muth, J. N., Bodi, I., Lewis, W., Varadi, G., and Schwartz, A. (2001) *Circulation* **103,** 140–147
31. Periasamy, M., Reed, T. D., Liu, L. H., Ji, Y., Loukianov, E., Paul, R. J., Nieman, M. L., Riddle, T., Duffy, J. J., Doetschman, T., Lorenz, J. N., and Shull, G. E. (1999) *J. Biol. Chem.* **274,** 2556–2562
32. He, H., Giordano, F. J., Hilal-Dandan, R., Choi, D. J., Rockman, H. A., McDonough, P. M., Bluhm, W. F., Meyer, M., Sayen, M. R., Swanson, E., and Dillmann, W. H. (1997) *J. Clin. Invest.* **100,** 380–389
33. Minamisawa, S., Hoshijima, M., Chu, G., Ward, C. A., Frank, K., Gu, Y., Martone, M. E., Wang, Y., Ross, J., Jr., Kranias, E. G., Giles, W. R., and Chien, K. R. (1999) *Cell* **99,** 313–322
34. Haimoto, H., and Kato, K. (1988) *Eur. J. Biochem.* **171,** 409–415
35. Zimmer, D. B. (1991) *Cell Motil. Cytoskelet.* **20,** 325–337
36. Fano, G., Angelella, P., Mariggio, D., Aisa, M. C., Giambanco, I., and Donato, R. (1989) *FEBS Lett.* **248,** 9–12
37. Kuo, W. N., Dominguez, J. L., Shabazz, K. A., White, D. J., Nicholson, J., Puente, K., Shells, P., Redding, C., Blake, T., and Sen, S. (1986) *Cytobios* **46,** 139–146
38. Tsoporis, J. N., Marks, A., Kahn, H. J., Butany, J. W., Liu, P. P., O'Hanlon, D., and Parker, T. G. (1998) *J. Clin. Invest.* **102,** 1609–1616
39. Wang, Z., Zhang, H., Ding, Y., Wang, G., Wang, X., Ye, S., Bartlam, M., Tang, H., Liu, Y., Jiang, F., Barraclough, R., Rudland, P. S., and Rao, Z. (2001) *Acta Crystallogr. Sect. D. Biol. Crystallogr.* **57,** 882–883
40. Drohat, A. C., Baldisseri, D. M., Rustandi, R. R., and Weber, D. J. (1998) *Biochemistry* **37,** 2729–2740
41. Lefkowitz, R. J., Rockman, H. A., and Koch, W. J. (2000) *Circulation* **101,** 1634–1637